

Effectivity of fluoride treatment on hydrogen and corrosion products generation in temporal implants for different magnesium alloys

Journal:	<i>Part H: Journal of Engineering in Medicine</i>
Manuscript ID:	JOEIM-13-0049
Manuscript Type:	Original article
Date Submitted by the Author:	22-Apr-2013
Complete List of Authors:	Trinidad, Javier; Mondragon Unibertsitatea, Mechanical and Manufacturing Department Arruebarrena, Gurutze; Mondragon Unibertsitatea, Mechanical and Manufacturing Department Marco, Iñigo; Mondragon Unibertsitatea, Mechanical and Manufacturing Department Hurtado, Iñaki; Mondragon Unibertsitatea, Mechanical and Manufacturing Department Sáenz de Argandoña, Eneko; Mondragon Unibertsitatea, Mechanical and Manufacturing Department
Keywords:	Magnesium, Biodegradation, Corrosion, Corrosion product, Surface treatment.
Abstract:	The increasing interest on magnesium alloys relies on their biocompatibility, bioabsorbability and especially on their mechanical properties. Due to these characteristics magnesium alloys are becoming a promising solution to be used, as temporary implants. However, magnesium alloys must overcome their poor corrosion resistance. This paper analyses the corrosion behaviour in PBS solution of three commercial magnesium alloys (AZ31B, WE43 and ZM21) as well as the influence of fluoride treatment on their corrosion behaviour. It is shown that the corrosion rate in all the alloys is decreased by fluoride treatment. However, fluoride treatment affects differently to each alloy.

SCHOLARONE™
Manuscripts

1
2
3
4
5
6
7
8
9 **Title:** Effectivity of fluoride treatment on hydrogen and corrosion products
10 generation in temporal implants for different magnesium alloys
11
12
13

14
15
16 **Authors:** Trinidad J., Arruebarrena G., Marco I., Hurtado I., Sáenz de Argandoña
17
18 E.
19

20
21
22
23 Trinidad J: *Tlf:* +34 943 73 96 55
24
25 *Fax:* +34 943 79 15 36
26
27 *e-mail:* jtrinidad@mondragon.edu
28

29
30 Arruebarrena G.: *Tlf:* +34 943 73 96 71
31
32 *Fax:* +34 943 79 15 36
33
34 *e-mail:* garruebarrena@mondragon.edu
35
36

37
38 Marco I.: *Tlf:* +34 943 73 96 55
39
40 *Fax:* +34 943 79 15 36
41
42 *e-mail:* inigo.marco@alumni.mondragon.edu
43
44

45
46 Hurtado I.: *Tlf:* +34 943 73 96 56
47
48 *Fax:* +34 943 79 15 36
49
50

1
2
3
4
5
6
7
8
9
10 *e-mail: ihurtado@mondragon.edu*

11 Sáenz de Argandoña E.: *Tlf: +34 943 71 19 06*

12
13
14 *Fax: +34 943 79 15 36*

15
16
17 *e-mail: esaenzdeargan@mondragon.edu*

18
19
20
21 **Affiliation:** Mechanical and Manufacturing Department. Mondragon Unibertsitatea.

22
23
24 Arrasate-Mondragon 20500 (Spain)

25
26
27
28 **Abstract**

29
30
31
32
33 The increasing interest on magnesium alloys relies on their biocompatibility,
34 bioabsorbility and especially on their mechanical properties. Due to these
35 characteristics magnesium alloys are becoming a promising solution to be used, as
36 temporary implants. However, magnesium alloys must overcome their poor
37 corrosion resistance. This paper analyses the corrosion behaviour in PBS solution
38 of three commercial magnesium alloys (AZ31B, WE43 and ZM21) as well as the
39 influence of fluoride treatment on their corrosion behaviour. It is shown that the
40
41
42
43
44
45
46
47
48
49
50

1
2
3
4
5
6
7
8
9 corrosion rate in all the alloys is decreased by fluoride treatment. However, fluoride
10 treatment affects differently to each alloy.
11
12

13
14
15
16 **Keywords:** Magnesium; Biodegradation; Corrosion; Corrosion product; Surface
17 treatment.
18
19

20 21 22 23 **1. Introduction** 24

25
26
27
28 The corrosion resistance and the high mechanical properties of some metallic
29 biomaterials make them very suitable to be used in long-term and load-bearing
30 applications [1, 2]. This way, metallic alloys such as Ti alloys, Co-Cr alloys and
31 stainless steels are commonly used materials in prosthesis, implants, plates or
32 screws.
33
34
35
36
37
38

39
40
41
42 On the other hand, novel medical applications and novel medical requirements are
43 demanding solutions beyond the state of the art. As an example, tissue
44 engineering, besides bioinert ability, demands bioabsorbable and bioactive
45
46
47
48
49
50

1
2
3
4
5
6
7
8
9 materials [3]. However, these properties, which were developed in ceramic and
10 polymer materials in the decade of the 80s, have not been achieved in metallic
11 materials yet. As a result, bioabsorbable metallic biomaterials have become an
12 attractive group of materials to be researched in recent years. This way, several
13 studies have been carried out with metallic bioabsorbable materials such as Mg
14 and its alloys [1, 4-19], Fe and Fe-Mn alloys [20, 21] and W [22-24].
15
16
17
18
19
20
21
22
23
24
25

26 Among the mentioned metallic materials, magnesium is the metal that is having a
27 greater impact on the scientific community, since it combines the property of being
28 compatible and absorbable by the human body and the property of accelerating
29 bone regeneration [4, 5]. In fact, most of the magnesium in the human body is in
30 the skeleton, being an essential component for bone growth and maturation [25,
31 26]. Regarding biocompatibility, magnesium is a biocompatible metallic material
32 representing the fourth most abundant cation in the body and the second most
33 important, after potassium, in the intracellular medium [27]. And finally, regarding its
34 ability to be bioabsorbed, the cations generated due to corrosion are efficiently
35 regulated by the body [15].
36
37
38
39
40
41
42
43
44
45
46
47
48
49
50
51
52
53
54
55
56
57
58
59
60

1
2
3
4
5
6
7
8
9
10
11
12 However, and as mentioned before, magnesium is not widely used in medical
13 applications yet due to its rapid corrosion in the organism [1, 4, 5, 28, 29]. The
14 corrosion of magnesium in physiological media generates hydroxides and
15 hydrogen (eq. 1). Depending on the corrosion rate, the hydroxides could alkalinize
16 the implant area [28] and the hydrogen generation could create subcutaneous gas
17 bubbles that could damage the tissue adjacent to the implantation site [4, 5]. As a
18 solution, a lower corrosion rate than the human body capacity to regulate
19 hydroxides and hydrogen would avoid both mentioned drawbacks.
20
21
22
23
24
25
26
27
28
29
30
31



38 A strategy to solve the rapid corrosion of magnesium is the application of surface
39 treatments [2, 14, 30-49]. One of the surface treatments most studied in literature
40 to improve the corrosion resistance of magnesium is the fluoride treatment [30-34,
41 50]. Fluoride treatment is a chemical conversion that consists on the immersion of
42 magnesium in hydrofluoric acid (HF) to form a coating of MgF_2 . The MgF_2 coating
43
44
45
46
47
48
49
50
51
52
53
54
55
56
57
58
59
60

1
2
3
4
5
6
7
8
9 presents a low water solubility and good biocompatibility [32, 33].
10
11

12
13
14 In the present work, the corrosion rate of three magnesium alloys widely used in
15 literature is evaluated: AZ31B [19, 30, 31, 50-54], WE43 [11, 19, 55-58] and ZM21
16 [59, 60]. This evaluation is carried out by measuring the hydrogen generation in
17 PBS solution. Furthermore and since a high adhesion of corrosion products on
18 magnesium surface could avoid the tissue growth in a cell culture, the corrosion
19 products generated during the degradation are also characterized.
20
21
22
23
24
25
26
27
28
29

30 **2. Experimental methods**

31 *2.1. Materials*

32
33
34
35
36
37
38
39
40 $10 \times 10 \times 1.5 \text{ mm}^3$ samples of commercial AZ31B (Magnesium Elektron, nominal
41 composition: 3 wt.% Al and 1 wt.% Zn), WE43 (Magnesium Elektron, nominal
42 composition: 4 wt.% Y and 3 wt.% rare earths), and ZM21 (Magnesium Elektron,
43 nominal composition: 2 wt.% Zn and 1 wt.% Mn) magnesium alloys were prepared.
44
45
46
47
48
49
50
51
52
53
54
55
56
57
58
59
60

1
2
3
4
5
6
7
8
9 The samples were ground with SiC papers from 1000 grits to 4000 grits,
10 ultrasonically rinsed in ethanol for 15 minutes and finally dried. 6 repetitions were
11 prepared for each material and surface treatment.
12
13
14
15
16
17

18 2.2. Fluoride treatment

19
20
21
22
23 To improve the corrosion resistance of magnesium alloys, the samples were
24 immersed in 48 wt.% concentration hydrofluoric acid (HF) solution for 24 hours and
25 72 hours under slow stirring to achieve the MgF₂ coating. MgF₂ coating was formed
26 by the reaction of HF with Mg, according to eq. (2) [61]. The treated samples were
27 ultrasonically rinsed in ethanol for 15 minutes and dried. The nomenclature used in
28 this work for each sample is described in table 1.
29
30
31
32
33
34
35
36
37
38
39



41
42
43
44
45 A maximum of 72 hours of immersion in HF was chosen in this work. According to
46 literature, Yan *et al.* [50] showed that after 72 hours in HF the coating thickness on
47
48
49
50
51

1
2
3
4
5
6
7
8
9 AZ31B alloy was not increased notoriously, neither the corrosion resistance. Yan *et*
10 *al.* [50] postulate that the formed barrier film of MgF_2 on the surface after 72 hours
11 was thick enough to terminate the reaction. Based on this previous research, and
12 in order to achieve comparable results, a maximum of 72 hours immersion in HF is
13 proposed for all the analysed alloys.
14
15
16
17
18
19

20 21 22 23 24 2.3. Immersion test 25 26 27

28 The samples were immersed in commercial PBS solution, which has been used for
29 magnesium implants evaluation in literature [32, 51, 62-67] and is recommended in
30 corrosion standards like ASTM F2129-08 or ASTM F746-04 for implants evaluation.
31 Dulbecco's Phosphate-Buffered Saline (D-PBS) (200 mg l^{-1} KCl, 200 mg l^{-1}
32 KH_2PO_4 , 8000 mg l^{-1} NaCl, 1150 mg l^{-1} Na_2HPO_4), was used with a starting pH of
33 7.4 at 37°C and without agitation. Approximately 40 ml of PBS per cm^2 sample
34 surface were used in order to avoid the change in the corrosivity of the media
35 according to ASTM G 31-72. Also the entire volume of PBS was changed every 48
36 hours to prevent the pH increase due to the generation of hydroxides.
37
38
39
40
41
42
43
44
45
46
47
48
49
50
51
52
53
54
55
56
57
58
59
60

1
2
3
4
5
6
7
8
9
10
11
12 The hydrogen evolution, as an indicator of the corrosion rate, was measured in a
13 eudiometer tube with a resolution of 0.1 ml. The procedure to measure the
14 corrosion is described by Song *et al.* [68].
15
16
17
18
19

20 21 *2.4. Characterisation of the fluoride coating and surface corrosion*

22
23
24
25

26 A scanning electron microscope was used for analysing the final morphology of the
27 samples. The energy dispersive X-ray (EDX) was used to analyse the coating and
28 the composition of depositions and corrosion products.
29
30
31
32
33
34

35 **3. Results**

36
37
38
39

40 *3.1. Fluoride treatment*

41
42
43
44

45 After fluoride treatment a stable film was formed on all the samples (figure 1). The
46 thickness of the coating increased with the immersion time for all the alloys. AZ31B
47
48
49
50

1
2
3
4
5
6
7
8
9 alloy presented a uniform film of 1.5 μm after 24 hours immersed in HF (figure 1a)
10 and grow to 2.5 μm after 72 hours immersed in HF (figure 1b). However, the
11 protected layer on the WE43 alloy was barely perceptible after 24 hours of
12 immersion. After 72 hour the film was not homogeneous and was clearly
13 concentrated in the intermetallics (figure 1d). In this thin film no cracks were
14 detected. Finally, the film on ZM21 alloy grows up to 2.8 μm in the first 24 hours
15 (figure 1e) and to 5 μm after 72 hours (figure 1f). Some cracks on the layer were
16 found.
17
18
19
20
21
22
23
24
25
26
27
28
29
30

31 Figure 1g shows the composition of the layer on the sample AZ31BHF72h after the
32 immersion. As it was expected the layer was rich in Mg and F indicating MgF_2
33 generation.
34
35
36
37
38
39

40 3.2. Immersion test

41
42
43
44

45 All magnesium alloys degraded during the immersion tests. In figure 2 hydrogen
46 evolution of the alloys during the immersion test is shown and it is also shown its
47
48
49
50
51
52
53
54
55
56
57
58
59
60

1
2
3
4
5
6
7
8
9 corrosion rate in order to get a better evaluation of the corrosion behaviour due to
10 pH changes. All the bare alloys revealed higher hydrogen generation during the
11 first 24 hours of the test with a decreasing and stabilizing corrosion rate over
12 increasing immersion time (figure 2). ZM21 bare alloy had the higher hydrogen
13 generation (0.0155 ml/mm² after 96 hours in PBS), followed by AZ31B (0.0109
14 ml/mm² after 96 hours in PBS) and WE43 (0.0093 ml/mm² after 96 hours in PBS).
15
16
17
18
19
20
21
22
23
24
25

26 Higher corrosion resistance was achieved for all the alloys after fluoride treatment.
27 However, fluoride treatment had a different influence in each magnesium alloy. This
28 way, and compared to bare alloys, the immersion of the samples in HF during 24
29 hours increased the corrosion resistance by 25% for AZ31B, 34% for ZM21 and
30 37% for WE43. Furthermore, the immersion of the samples in HF during 72 hours
31 increased the corrosion resistance by 50% for WE43, 52% for AZ31B and 75% for
32 ZM21. ZM21HF72h sample showed the lowest hydrogen generation (0.0039
33 ml/mm² after 96 hours in PBS) of all the samples. The corrosion rate evolution for
34 all the bare alloys is shown in figure 2.
35
36
37
38
39
40
41
42
43
44
45
46
47
48
49
50
51
52
53
54
55
56
57
58
59
60

1
2
3
4
5
6
7
8
9
10 In contrast to bare alloys, coated alloys started with a low corrosion rate and it
11 increased slightly over immersion time due to magnesium fluoride film dissolution
12 (figure 2). It was also observed that fluoride treatment made the alloys to show less
13 dispersion in the results from sample to sample (figure 2).
14
15
16
17

18
19
20
21 There were not significant pH variations (table 2). However, the corrosion rate in
22 the samples did show small changes due to these pH changes (figure 2).
23
24
25
26
27

28 *3.3. Characterisation of the surface corrosion*

29
30
31

32
33 The morphological features of the samples after an immersion in PBS for 72 hours
34 are shown in figure 3. The highest adhesion of precipitates was observed on
35 AZ31B (figure 3a) alloy. WE43 (figure 3d) and ZM21 (figure 3g) alloys presented
36 less activity. In all cases, the fluoride treatment decreased the adhesion of crystals
37 to the surface (figure 3).
38
39
40
41
42
43
44

45
46
47 Furthermore, in figure 3c and figure 3g some small black depositions were
48
49
50

1
2
3
4
5
6
7
8
9 detected. As shown in figure 4, these particles are rich in C, Mg and O.
10
11

12
13
14 Regarding the beginning of the corrosion, figure 5 shows the start of a corrosion
15 point on AZ31B alloy. The distribution maps showed the presence of O, P, and Ca.
16 Also the influence of Cl was detected on the surface. Longer immersion test in PBS
17 of bare alloys give as a result the presence of several formations. After 7 days of
18 immersion, needle like depositions rich in Mg, K, P, Na, K and O (figure 6) and
19 sponge-like depositions rich in Mg, P, Ca, Na, K and O (figure 7) were adhered on
20 AZ31B sample surface. In ZM21 samples depositions rich in Mg, P and O were
21 also adhered but in more localized areas (figure 8). In the case of WE43 bare alloy
22 no significant adhesions were found.
23
24
25
26
27
28
29
30
31
32
33
34
35
36
37

38 Regarding the beginning of the corrosion in coated alloys, figure 9 shows the start
39 of the corrosion on AZ31B alloy with a fluoride treatment of 24 hours. After MgF_2
40 dissolution, corrosion point becomes richer in O, P, Na and Ca. For AZ31BHF72h
41 and for coated WE43 and ZM21 alloys no significant formations were found.
42
43
44
45
46
47
48
49
50
51
52
53
54
55
56
57
58
59
60

4. Discussion

The corrosion of three different magnesium alloys under the same conditions has been compared in the present work. The results are compared with literature in table 3. The first conclusion when analysing the literature is the high dispersion of the results achieved by different authors. There may be many reasons for this dispersion but the most important one is the lack of standardisation [65] and, in the cases when potentiodynamic polarisation is used, the inability of Tafel extrapolation to estimate the corrosion rate reliably [6, 7, 68]. Nevertheless, the results achieved in the present research work fit with the results achieved by other authors as shown next.

First, a comparison of the bare alloys is carried out. In the case of AZ31B magnesium alloy, the corrosion rate measured by other authors moves between 0.25 and 2 mm year⁻¹. The corrosion rate for AZ31B measured in this work, 0.56 mm year⁻¹, is between literature values and close to the results measured *in vivo*, 0.672 mm year⁻¹ [70]. In the case of WE43 magnesium alloy, the corrosion rate

1
2
3
4
5
6
7
8
9 measured by other authors moves between 0.3 and 1.5 mm year⁻¹. As happened
10 with the previous mentioned alloy, the corrosion rate of WE43 measured at the
11 present research work, 0.47 mm year⁻¹, is between literature values. However, in
12 the case of WE43 magnesium alloy, the *in vivo* corrosion rate measured by other
13 authors is greater, 0.704 mm year⁻¹ [56], 0.896 mm year⁻¹ [70], 1.44 mm year⁻¹
14 [56]. Finally, not many works with ZM21 magnesium alloy were found in literature.
15 However, and as shown in table 3, the most common measured corrosion rate for
16 ZM21 is around 0.9 mm year⁻¹ and the corrosion rate measured at the present
17 research work is 0.79 mm year⁻¹, close to the literature values.
18
19
20
21
22
23
24
25
26
27
28
29
30
31
32

33 Regarding the coating treatment, the corrosion resistance of all magnesium alloys
34 was increased by fluoride treatment. Longer fluoride treatment resulted in lower
35 hydrogen generation. Therefore, a positive influence of the fluoride treatment on
36 the magnesium corrosion was observed as stated previously [30-34, 50]. Cracks
37 were found on ZM21HF24h and ZM21HF72h samples, and also sporadically on
38 AZ31BHF72h sample, where thicker layers were generated during the fluoride
39 treatment. On the other hand, no cracks were found in the others samples where
40
41
42
43
44
45
46
47
48
49
50
51
52
53
54
55
56
57
58
59
60

1
2
3
4
5
6
7
8
9 thinner layers were created. The cracks may have appeared due to the brittleness
10 of the coating [75] in samples with a thick layer.
11
12
13

14
15
16 The increase of the corrosion resistance by fluoride treatment depends on the
17 morphology of the coating generated for each alloy (figure 1). In the case of the
18 AZ31B and ZM21 magnesium alloys this dependency is clearer. For both alloys,
19 the greater the coating thickness is, the greater the corrosion protection it offers.
20
21 AZ31BHF24h, with a coating thickness of 1.5 μm , shows a corrosion rate 25%
22 smaller than the untreated AZ31B magnesium alloy. AZ31BHF72h, with a coating
23 thickness of 2.5 μm , shows a corrosion rate 52% smaller than the untreated AZ31B
24 magnesium alloy. In the case of ZM21 magnesium alloy, the ZM21HF24h with a
25 coating thickness of 2.8 μm shows a corrosion rate 34% smaller than the untreated
26 ZM21 magnesium alloy and the ZM21HF72h with a coating thickness of 5 μm
27 shows a corrosion rate 75% smaller than the untreated ZM21 magnesium alloy.
28
29 The tendency towards greater protection when the fluoride treatment is longer is
30 also proved for the WE43 magnesium alloy. WE43HF24h shows a corrosion rate
31 37% smaller than the untreated alloy and the WE43HF72h shows a corrosion rate
32
33
34
35
36
37
38
39
40
41
42
43
44
45
46
47
48
49
50
51
52
53
54
55
56
57
58
59
60

1
2
3
4
5
6
7
8
9 50% smaller than the untreated alloy. However, unlike AZ31B and ZM21 alloys,
10 there is no a direct relation between the corrosion rate decrement and the coating
11 thickness for WE43 magnesium alloy: the coating on WE43HF24h was barely
12 perceptible and WE43HF72h presented a non-uniform coating.
13
14
15
16
17
18
19

20
21 Despite WE43 alloy did not present a homogeneous coating it achieved the highest
22 reduction in corrosion rate (37%) after 24 hours of immersion in HF. The
23 explanation for this may be that micro-galvanic corrosion occurs in magnesium
24 alloys with rare earth [76]. As mentioned before, the coating concentrated around
25 the intermetallics, leaving α -Mg almost without protection. Therefore this
26 encapsulation could have eliminated the micro-galvanic couples between α -Mg and
27 the intermetallics thereby increasing the corrosion resistance of the alloy.
28
29
30
31
32
33
34
35
36
37
38
39

40 In order to analyse the possibility of form a thicker coating on α -Mg of WE43 alloy,
41 samples were immersed in HF during 168 hours. The coating on these samples
42 was also non uniform and barely appreciable in some areas (figure 10). This figure
43 also shows that the coating concentrates around the intermetallics. This effect
44
45
46
47
48
49
50
51
52
53
54
55
56
57
58
59
60

1
2
3
4
5
6
7
8
9 could disappear dissolving the intermetallics in a heat treatment before fluoride
10 treatment.
11
12

13
14
15
16 After 72 hours of immersion in PBS, MgF_2 coating was still present on the all
17 sample surface, especially in ZM21 alloy. Regarding the adhesion of corrosion
18 products to the surface, WE43 alloy was the one that showed the lowest adhesion.
19
20 Nevertheless, the adhesion in the other magnesium alloys is decreased with
21 fluoride treatment. In the case of AZ31, as shown in figure 3, the adhesion of
22 crystals decreased dramatically after fluoride treatment.
23
24
25
26
27
28
29
30
31
32

33 The elemental analysis suggests that, at the beginning of the corrosion, a mixture
34 of MgCl_2 and $\text{Mg}(\text{OH})_2$ could be the predominant species in the corrosion of bare
35 alloys. The formed $\text{Mg}(\text{OH})_2$ could be dissolved in aqueous medium and
36 transformed into soluble MgCl_2 by chloride ions [66]. As corrosion progresses, the
37 elemental analysis suggests that different phosphates $(\text{PO}_4)^{3-}$ with Mg, Ca, K or Na
38 were deposited on the surface. Depositions or corrosion products containing
39
40
41
42
43
44
45
46
47
48
49
50
51
52
53
54
55
56
57
58
59
60
 $(\text{PO}_4)^{3-}$ are also detected in others works [51, 77, 78]. Finally, some $(\text{CO}_3)^{2-}$

1
2
3
4
5
6
7
8
9 particles (figure 4) were also detected. The presence of carbonates are common
10 after the immersion of magnesium in physiological medium [54, 59, 77], however,
11 in this work there were no many of carbonate because PBS does not contain any.
12
13 Nevertheless the presence of some could be explained due to the reaction of
14 distilled water with the CO₂ of the atmosphere. In the same way, although PBS
15 does not contain Ca, elemental analysis detected small amounts of Ca. In this
16 case, it may be found as an impurity in PBS.
17
18
19
20
21
22
23
24
25
26
27

28 **5. Conclusions**

- 29
30
31
32
33 (i) Immersion tests in PBS showed an improved corrosion rate, ranging from
34 25% for AZ31B alloy after 24 hours in HF to 75% for ZM21 alloy after 72
35 hours in HF, and a reduced corrosion products and crystals adhesion for the
36 coated alloys compared to the bare alloys.
37
38 (ii) For all the alloys it was stated that the corrosion rate depends on the
39 immersion time in HF, higher immersion times offer lower corrosion rates.
40
41 (iii) Morphology and formed MgF₂ thickness depend on alloy microstructure. In
42
43
44
45
46
47
48
49
50
51
52
53
54
55
56
57
58
59
60

1
2
3
4
5
6
7
8
9 the case of WE43, MgF₂ was concentrated on intermetallics and coating
10 was not homogeneous. On the other hand, for AZ31B and ZM21 alloy the
11 coating thickness was proportional to the fluoride treatment time.
12
13
14
15

16 (iv) There is not a direct relation between the coating thickness and the
17 corrosion protection achieved in all the alloys. In the case of the ZM21 and
18 AZ31B alloys this direct relation has been found. However, in the case of the
19 WE43 alloy even very thin protection layers generates high corrosion
20 protection.
21
22
23
24
25
26
27
28
29
30

31 **Acknowledgements**

32
33
34
35 This work was supported by the Department of Industry, Innovation, Trade and
36 Tourism of the Basque Government through the SAIOTEK program and by the
37 Ministry of Science and Innovation of the Government of Spain through the PSE-
38 010000-2009-3 of the PSE program.
39
40
41
42
43
44
45

46 **References**

- 1
2
3
4
5
6
7
8
9
10
11
12 [1] Staiger MP, Pietak AM, Huadmai J, Dias G. Magnesium and its alloys as
13 orthopedic biomaterials: A review. *Biomaterials*. 2006; 27(9):1728–1734.
14
15
16 [2] Wong HM, Yeung KWK, Lam KO, Tam V, Chu PK, Luk KDK, *et al.* A
17 biodegradable polymer-based coating to control the performance of
18 magnesium alloy orthopaedic implants. *Biomaterials*. 2010; 31(8):2084–2096.
19
20
21 [3] Hench LL, Polak JM. Third-generation biomedical materials. *Science*. 2002;
22 295(5557):1014+1016–1017.
23
24
25 [4] Witte F, Ulrich H, Rudert M, Willbold E. Biodegradable magnesium scaffolds:
26 Part I: Appropriate inflammatory response. *Journal of Biomedical Materials*
27 *Research - Part A*. 2007; 81(3):748–756.
28
29
30 [5] Witte F, Ulrich H, Palm C, Willbold E. Biodegradable magnesium scaffolds:
31 Part II: Peri-implant bone remodeling. *Journal of Biomedical Materials*
32 *Research - Part A*. 2007; 81(3):757–765.
33
34
35 [6] Atrens A, Liu M, Abidin NIZ. Corrosion mechanism applicable to
36 biodegradable magnesium implants. *Materials Science and Engineering: B*.
37 2011; 176(20):1609–1636.
38
39
40
41
42
43
44
45
46
47
48
49
50
51
52
53
54
55
56
57
58
59
60

- 1
2
3
4
5
6
7
8
9
10 [7] Shi Z, Liu M, Atrens A. Measurement of the corrosion rate of magnesium
11 alloys using Tafel extrapolation. *Corrosion Science*. 2010; 52(2):579–588.
12
13
14 [8] Shi Z, Atrens A. An innovative specimen configuration for the study of Mg
15 corrosion. *Corrosion Science*. 2011; 53(1):226–246.
16
17
18 [9] Shi Z, Jia JX, Atrens A. Galvanostatic anodic polarisation curves and galvanic
19 corrosion of high purity Mg in 3.5 *Corrosion Science*. 2012; 60(0):296–308.
20
21
22
23 [10] Qiao Z, Shi Z, Hort N, Abidin NIZ, Atrens A. Corrosion behaviour of a
24 nominally high purity Mg ingot produced by permanent mould direct chill
25 casting. *Corrosion Science*. 2012; 61(0):185–207.
26
27
28
29 [11] Gu X, Zheng Y, Cheng Y, Zhong S, Xi T. *In vitro* corrosion and biocompatibility
30 of binary magnesium alloys. *Biomaterials*. 2009; 30(4):484–498.
31
32
33
34 [12] Gu X, Zheng Y, Zhong S, Xi T, Wang J, Wang W. Corrosion of, and cellular
35 responses to Mg-Zn-Ca bulk metallic glasses. *Biomaterials*. 2010;
36
37
38
39
40
41
42
43 [13] Kannan MB, Raman RKS. *In vitro* degradation and mechanical integrity of
44 calcium-containing magnesium alloys in modified-simulated body fluid.
45
46
47
48
49
50
51
52
53
54
55
56
57
58
59
60

- 1
2
3
4
5
6
7
8
9 [14] Li J, Song Y, Zhang S, Zhao C, Zhang F, Zhang X, *et al.* *In vitro* responses of
10 human bone marrow stromal cells to a fluoridated hydroxyapatite coated
11 biodegradable Mg-Zn alloy. *Biomaterials*. 2010; 31(22):5782–5788.
12
13
14
15
16 [15] Li Z, Gu X, Lou S, Zheng Y. The development of binary Mg-Ca alloys for use
17 as biodegradable materials within bone. *Biomaterials*. 2008; 29(10):1329–
18 1344.
19
20
21
22
23 [16] Peng Q, Huang Y, Zhou L, Hort N, Kainer KU. Preparation and properties of
24 high purity Mg-Y biomaterials. *Biomaterials*. 2010; 31(3):398–403.
25
26
27
28 [17] Witte F, Feyerabend F, Maier P, Fischer J, Stormer M, Blawert C, *et al.*
29 Biodegradable magnesium-hydroxyapatite metal matrix composites.
30 *Biomaterials*. 2007; 28(13):2163–2174.
31
32
33
34 [18] Witte F, Fisher J, Nellesen J, Crostack HA, Kaese V, Pisch A, *et al.* *In vitro*
35 and *in vivo* corrosion measurements of magnesium alloys. *Biomaterials*.
36 2006; 27(7):1013-1018.
37
38
39
40
41
42 [19] Witte F, Kaese V, Haferkamp H, Switzer E, Meyer-Lindenberg A, Wirth CJ, *et*
43 *al.* *In vivo* corrosion of four magnesium alloys and the associated bone
44 response. *Biomaterials*. 2005; 26(17):3557-3563.
45
46
47
48
49
50
51
52
53
54
55
56
57
58
59
60

- 1
2
3
4
5
6
7
8
9
10 [20] Hermawan H, Dubé D, Mantovani D. Degradable metallic biomaterials:
11 Design and development of Fe-Mn alloys for stents. *Journal of Biomedical*
12 *Materials Research Part A*. 2010; 93A(1):1–11.
13
14
15
16 [21] Hermawan H, Purnama A, Dubé D, Couet J, Mantovani D. Fe-Mn alloys for
17 metallic biodegradable stents: Degradation and cell viability studies. *Acta*
18 *Biomaterialia*. 2010; 6(5):1852–1860.
19
20
21
22 [22] Peuster M, Fink C, Wohlsein P, Bruegmann M, Gunther A, Kaese V, *et al.*
23 Degradation of tungsten coils implanted into the subclavian artery of New
24 Zealand white rabbits is not associated with local or systemic toxicity.
25 *Biomaterials*. 2003; 24(3):393–399.
26
27
28 [23] Peuster M, Fink C, Von Schnakenburg C. Biocompatibility of corroding
29 tungsten coils: *In vitro* assessment of degradation kinetics and cytotoxicity on
30 human cells. *Biomaterials*. 2003; 24(22):4057–4061.
31
32
33 [24] Peuster M, Kaese V, Wuensch G, Von Schnakenburg C, Niemeyer M, Fink C,
34 *et al.* Composition and *In Vitro* Biocompatibility of Corroding Tungsten Coils.
35 *Journal of Biomedical Materials Research - Part B Applied Biomaterials*.
36
37
38
39
40
41
42
43
44
45
46
47
48
49
50
51
52
53
54
55
56
57
58
59
60

- 1
2
3
4
5
6
7
8
9 [25] Aranda P, Planells E, Llopis J. Magnesio. *Ars Pharmaceutica*. 2000; 41(1):91-
10 100.
11
12
13
14 [26] Iannello S, Belfiore F. Hypomagnesemia. A review of pathophysiological,
15 clinical and therapeutical aspects. *Panminerva Medica*. 2001; 43(3):177-209.
16
17
18 [27] Gums J. Magnesium in cardiovascular and other disorders. *American Journal*
19 *of Health-System Pharmacy*. 2004; 61(15):1569-1576.
20
21
22
23 [28] Zeng R, Dietzel W, Witte F, Hort N, Blawert C. Progress and challenge for
24 magnesium alloys as biomaterials. *Advanced Engineering Materials*. 2008;
25 10(8):B3–B14.
26
27
28 [29] Pietak A, Mahoney P, Dias GJ, Staiger MP. Bone-like matrix formation on
29 magnesium and magnesium alloys. *Journal of Materials Science: Materials in*
30 *Medicine*. 2008; 19(1):407–415.
31
32
33 [30] da Conceicao TF, Scharnagl N, Dietzel W, Hoeche D, Kainer KU. Study on
34 the interface of PVDF coatings and HF-treated AZ31 magnesium alloy:
35 Determination of interfacial interactions and reactions with selfhealing
36 properties. *Corrosion Science*. 2011; 53(2):712–719.
37
38
39
40
41
42
43
44
45
46
47 [31] Carboneras M, Garcia-Alonso MC, Escudero ML. Biodegradation kinetics of
48
49
50
51
52
53
54
55
56
57
58
59
60

- 1
2
3
4
5
6
7
8
9 modified magnesium-based materials in cell culture medium. *Corrosion*
10
11 *Science*. 2011; 53(4):1433–1439.
12
13
- [32] Pereda MD, Alonso C, Burgos-Asperilla L, del Valle JA, Ruano OA, Perez P,
14
15 *et al.* Corrosion inhibition of powder metallurgy Mg by fluoride treatments.
16
17 *Acta Biomaterialia*. 2010; 6(5):1772–1782.
18
19
- [33] Pereda MD, Alonso C, Gamero M, del Valle JA, de Mele MFL. Comparative
20
21 study of fluoride conversion coatings formed on biodegradable powder
22
23 metallurgy Mg: The effect of chlorides at physiological level. *Materials*
24
25 *Science and Engineering C*. 2011; 31(5):858–865.
26
27
28
29
- [34] Witte F, Fischer J, Nellesen J, Vogt C, Vogt J, Donath T, *et al.* *In vivo*
30
31 corrosion and corrosion protection of magnesium alloy LAE442. *Acta*
32
33 *Biomaterialia*. 2010; 6(5):1792–1799.
34
35
36
37
- [35] Chen S, Guan S, Chen B, Li W, Wang J, Wang L, *et al.* Corrosion behavior of
38
39 TiO₂ films on Mg-Zn alloy in simulated body fluid. *Applied Surface Science*.
40
41 2011; 257(9):4464–4467.
42
43
44
- [36] Chen XB, Birbilis N, Abbott TB. A simple route towards a hydroxyapatite-
45
46 Mg(OH)₂ conversion coating for magnesium. *Corrosion Science*. 2011;
47
48
49
50
51
52
53
54
55
56
57
58
59
60

- 1
2
3
4
5
6
7
8
9 53(6):2263–2268.
- 10
11 [37] Gao JH, Guan SK, Chen J, Wang LG, Zhu SJ, Hu JH, *et al.* Fabrication and
12 characterization of rod-like nano-hydroxyapatite on MAO coating supported
13 on Mg-Zn-Ca alloy. *Applied Surface Science*. 2010; 257(6):2231–2237.
- 14
15
16
17
18 [38] Hahn BD, Park DS, Choi JJ, Ryu J, Yoon WH, Choi JH, *et al.* Aerosol
19 deposition of hydroxyapatite-chitosan composite coatings on biodegradable
20 magnesium alloy. *Surface and Coatings Technology*. 2011; 205(8-9):3112–
21 3118.
- 22
23
24
25
26
27
28 [39] Hiromoto S, Yamamoto A. Control of degradation rate of bioabsorbable
29 magnesium by anodization and steam treatment. *Materials Science and*
30 *Engineering C*. 2010; 30(8):1085–1093.
- 31
32
33
34
35 [40] Keim S, Brunner JG, Fabry B, Virtanen S. Control of magnesium corrosion
36 and biocompatibility with biomimetic coatings. *Journal of Biomedical Materials*
37 *Research - Part B Applied Biomaterials*. 2011; 96 B(1):84–90.
- 38
39
40
41
42 [41] Li JN, Cao P, Zhang XN, Zhang SX, He YH. *In vitro* degradation and cell
43 attachment of a PLGA coated biodegradable Mg-6Zn based alloy. *Journal of*
44 *Materials Science*. 2010; 45(22):6038–6045.
- 45
46
47
48
49
50
51
52
53
54
55
56
57
58
59
60

- 1
2
3
4
5
6
7
8
9
10 [42] Li M, Chen Q, Zhang W, Hu W, Su Y. Corrosion behavior in SBF for titania
11 coatings on Mg-Ca alloy. *Journal of Materials Science*. 2011; 46(7):2365–
12 2369.
13
14
15
16 [43] Liu GY, Hu J, Ding ZK, Wang C. Bioactive calcium phosphate coating formed
17 on micro-arc oxidized magnesium by chemical deposition. *Applied Surface*
18 *Science*. 2010; 257(6):2051–2057.
19
20
21
22
23 [44] Lu P, Cao L, Liu Y, Xu X, Wu X. Evaluation of magnesium ions release,
24 biocorrosion, and hemocompatibility of MAO/PLLA-modified magnesium alloy
25 WE42. *Journal of Biomedical Materials Research - Part B Applied*
26 *Biomaterials*. 2011; 96 B(1):101–109.
27
28
29
30
31
32
33 [45] Ma C, Zhang X, Qu L, Li M. Calcium and Phosphate Biocoatings on
34 Magnesium Alloy Fabricated By Micro-arc Oxidation. *Advanced Materials*
35 *Research*. 2010; 105-106:565–568.
36
37
38
39
40 [46] Song Y, Zhang S, Li J, Zhao C, Zhang X. Electrodeposition of Ca-P coatings
41 on biodegradable Mg alloy: *In vitro* biomineralization behavior. *Acta*
42 *Biomaterialia*. 2010; 6(5):1736–1742.
43
44
45
46
47 [47] Song YW, Shan DY, Han EH. Electrodeposition of hydroxyapatite coating on
48
49
50
51
52
53
54
55
56
57
58
59
60

- 1
2
3
4
5
6
7
8
9 AZ91D magnesium alloy for biomaterial application. *Materials Letters*. 2008;
10 62(17-18):3276–3279.
11
12
13
14 [48] Xu L, Pan F, Yu G, Yang L, Zhang E, Yang K. *In vitro* and *in vivo* evaluation of
15 the surface bioactivity of a calcium phosphate coated magnesium alloy.
16 *Biomaterials*. 2009; 30(8):1512–1523.
17
18
19 [49] Xu L, Zhang E, Yang K. Phosphating treatment and corrosion properties of
20 Mg-Mn-Zn alloy for biomedical application. *Journal of Materials Science:*
21 *Materials in Medicine*. 2009; 20(4):859–867.
22
23
24 [50] Yan T, Tan L, Xiong D, Liu X, Zhang B, Yang K. Fluoride treatment and *in vitro*
25 corrosion behavior of an AZ31B magnesium alloy. *Materials Science and*
26 *Engineering C*. 2010; 30(5):740–748.
27
28
29 [51] Alvarez-Lopez M, Pereda MD, del Valle JA, Fernandez-Lorenzo M, Garcia-
30 Alonso MC, Ruano OA, *et al*. Corrosion behaviour of AZ31 magnesium alloy
31 with different grain sizes in simulated biological fluids. *Acta Biomaterialia*.
32 2010; 6(5):1763–1771.
33
34
35 [52] Ghoneim AA, Fekry AM, Ameer MA. Electrochemical behavior of magnesium
36 alloys as biodegradable materials in Hank's solution. *Electrochimica Acta*.
37
38
39
40
41
42
43
44
45
46
47
48
49
50
51
52
53
54
55
56
57
58
59
60

- 1
2
3
4
5
6
7
8
9 2010; 55(20):6028–6035.
- 10
11 [53] Kim YK, Lee MH, Prasad MN, Park IS, Lee MH, Seol KW, *et al.* Surface
12 characteristics of magnesium alloys treated by anodic oxidation using pulse
13 power. *Advanced Materials Research*. 2008; 47-50:1290–1293.
- 14
15
16 [54] Qu Q, Ma J, Wang L, Li L, Bai W, Ding Z. Corrosion behaviour of AZ31B
17 magnesium alloy in NaCl solutions saturated with CO₂. *Corrosion Science*.
18 2011; 53(4):1186–1193.
- 19
20
21 [55] Gu XN, Zhou WR, Zheng YF, Cheng Y, Wei SC, Zhong SP, *et al.* Corrosion
22 fatigue behaviors of two biomedical Mg alloys - AZ91D and WE43 - In
23 simulated body fluid. *Acta Biomaterialia*. 2010; 6(12):4605–4613.
- 24
25
26 [56] Krause A, von der Hoh N, Bormann D, Krause C, Bach FW, Windhagen H, *et*
27 *al.* Degradation behaviour and mechanical properties of magnesium implants
28 in rabbit tibiae. *Journal of Materials Science*. 2010; 45(3):624–632.
- 29
30
31 [57] Wu W, Petrini L, Gastaldi D, Villa T, Vedani M, Lesma E, *et al.* Finite element
32 shape optimization for biodegradable magnesium alloy stents. *Annals of*
33 *Biomedical Engineering*. 2010; 38(9):2829–2840.
- 34
35
36 [58] Xu L, Zhang E, Yin D, Zeng S, Yang K. *In vitro* corrosion behaviour of Mg
37
38
39
40
41
42
43
44
45
46
47
48
49
50
51
52
53
54
55
56
57
58
59
60

- 1
2
3
4
5
6
7
8
9 alloys in a phosphate buffered solution for bone implant application. Journal
10 of Materials Science. 2008; 19(3):1017-1025.
11
12
13
14 [59] Jamesh M, Kumar S, Narayanan TSNS. Corrosion behavior of commercially
15 pure Mg and ZM21 Mg alloy in Ringer's solution - Long term evaluation by
16 EIS. Corrosion Science. 2011; 53(2):645–654.
17
18
19
20
21 [60] Erinc M, Sillekens WH, Mannens RGTM, Werkhoven RJ. Applicability of
22 existing magnesium alloys as biomedical implant materials. In: Magnesium
23 Technology. San Francisco, CA, United states; 2009, 209-214.
24
25
26
27
28 [61] da Conceicao TF, Scharnagl N, Dietzel W, Kainer KU. On the degradation
29 mechanism of corrosion protective poly(ether imide) coatings on magnesium
30 AZ31 alloy. Corrosion Science. 2010; 52(10):3155–3157.
31
32
33
34
35 [62] Aghion E, Yered T, Perez Y, Gueta Y. The prospects of carrying and releasing
36 drugs via biodegradable magnesium foam. Advanced Engineering Materials.
37 2010; 12(8):B374–B379.
38
39
40
41
42 [63] Alonso C, del Valle JA, Gamero M, de Mele MFL. Do phosphate ions affect
43 the biodegradation rate of fluoride-treated Mg? Materials Letters. 2012;
44 68(0):149–152.
45
46
47
48
49
50
51
52
53
54
55
56
57
58
59
60

- 1
2
3
4
5
6
7
8
9
10 [64] Hänzi AC, Gerber I, Schinhammer M, Lffler JF, Uggowitzer PJ. On the *in vitro*
11 and *in vivo* degradation performance and biological response of new
12 biodegradable Mg-Y-Zn alloys. *Acta Biomaterialia*. 2010; 6(5):1824–1833.
13
14
15
16 [65] Mueller WD, Nascimento ML, de Mele MFL. Critical discussion of the results
17 from different corrosion studies of Mg and Mg alloys for biomaterial
18 applications. *Acta Biomaterialia*. 2010; 6(5):1749–1755.
19
20
21
22
23 [66] Xin Y, Hu T, Chu PK. *In vitro* studies of biomedical magnesium alloys in a
24 simulated physiological environment: A review. *Acta Biomaterialia*. 2011;
25 7(4):1452–1459.
26
27
28
29
30 [67] Xue D, Yun Y, Tan Z, Dong Z, Schulz MJ. *In Vivo* and *In Vitro* Degradation
31 Behavior of Magnesium Alloys as Biomaterials. *Journal of Materials Science*
32 & Technology. 2012; 28(3):261–267.
33
34
35
36
37 [68] Song G, Atrens A. Understanding magnesium corrosion. A framework for
38 improved alloy performance. *Advanced Engineering Materials*. 2003;
39 5(12):837–858.
40
41
42
43
44 [69] Schille C, Reichel HP, Hort N, Geis-Gerstorfer J. Corrosion of Experimental
45 Magnesium Alloys for use as a Possible Bone Replacement Material. In:
46
47
48
49
50
51
52
53
54
55
56
57
58
59
60

- 1
2
3
4
5
6
7
8
9
10 Magnesium: 8th International Conference on Magnesium Alloys and their
11 Applications. Weinheim, Germany; 2010; 1195-1200.
- 12
13
14 [70] Gu X, Zheng Y. A review on magnesium alloys as biodegradable materials.
15
16 Frontiers of Materials Science in China. 2010; 4(2):111-115.
- 17
18 [71] Ren Y, Huang J, Zhang B, Yang K. Preliminary study of biodegradation of
19
20 AZ31B magnesium alloy. Front Mater Sci. 2007; 1(4):401-404.
- 21
22
23 [72] Tan LL, Wang Q, Geng F, Xi XS, Qiu JH, Yang K. Preparation and
24
25 characterization of Ca-P coating on AZ31 magnesium alloy. Transactions of
26
27 Nonferrous Metals Society of China (English Edition). 2010; 20(SUPPL.
28
29 2):s648–s654.
- 30
31
32 [73] Wang H, Shi ZM, Yang K. Magnesium and Magnesium Alloys as Degradable
33
34 Metallic Biomaterials. Advanced Materials Research. 2008; 32:207-210.
- 35
36
37 [74] Wen Z, Wu C, Dai C, Yang F. Corrosion behaviors of Mg and its alloys with
38
39 different Al contents in a modified simulated body fluid. Journal of Alloys and
40
41 Compounds. 2010; 488(1):392–399.
- 42
43
44 [75] Seitz JM, Collier K, Wulf E, Bormann D, Bach FW. Comparison of the
45
46 Corrosion Behavior of Coated and Uncoated Magnesium Alloys in an *In Vitro*
47
48
49
50
51
52
53
54
55
56
57
58
59
60

1
2
3
4
5
6
7
8
9 Corrosion Environment. *Advanced Engineering Materials*. 2011; 13(9):B313–
10 B323.

- 11
12
13
14 [76] Coy AE, Viejo F, Skeldon P, Thompson GE. Susceptibility of rare-earth
15 magnesium alloys to micro-galvanic corrosion. *Corrosion Science*. 2010;
16 52(12):3896–3906.
17
18
19
20
21 [77] Tie D, Feyerabend F, Hort N, Willumeit R, Hoeche D. XPS studies of
22 magnesium surfaces after exposure to Dulbecco's modified eagle medium,
23 Hank's buffered salt solution, and simulated body fluid. Vol. 12. P.O. Box
24 101161, Weinheim, D-69451, Germany; 2010. p. B699–B704.
25
26
27
28
29
30
31 [78] Zhang S, Zhang X, Zhao C, Li J, Song Y, Xie C, *et al.* Research on an Mg-Zn
32 alloy as a degradable biomaterial. *Acta Biomaterialia*. 2010; 6(2):626–640.
33
34
35
36
37
38
39
40
41
42
43
44
45
46
47
48
49
50
51
52
53
54
55
56
57
58
59
60

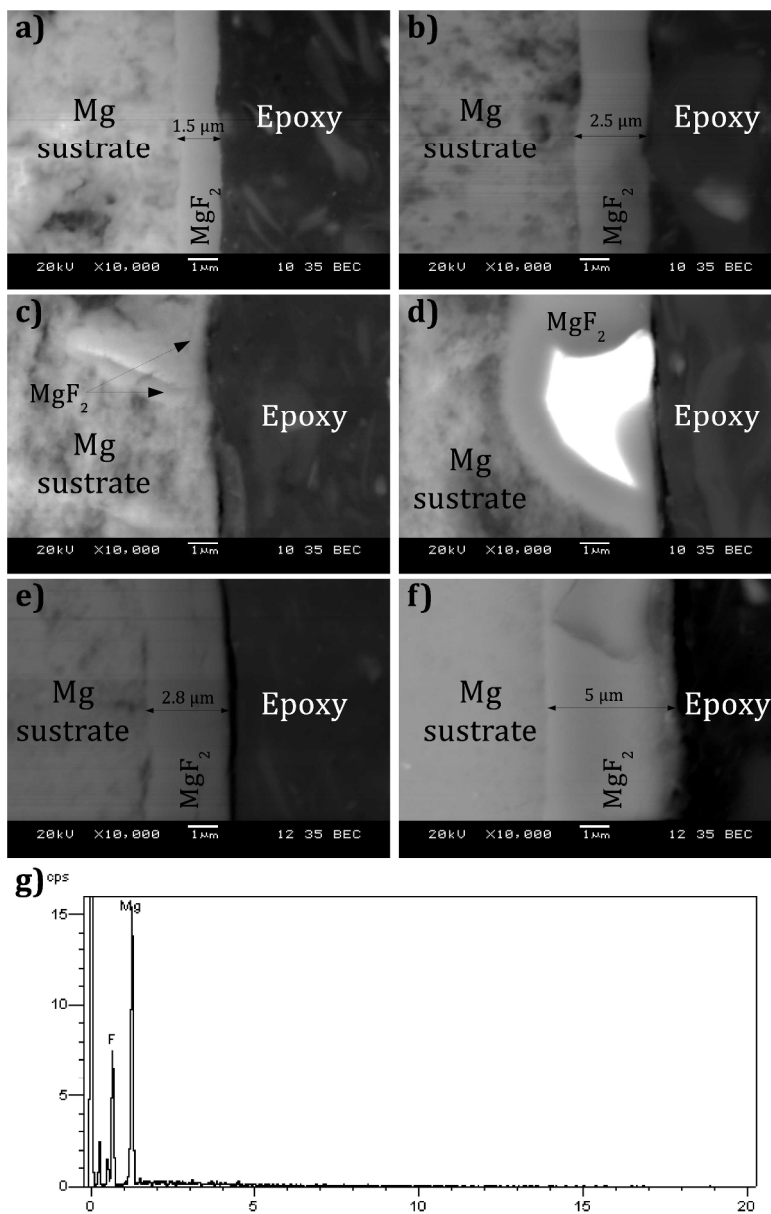


Figure 1: Detail of the thickness of the different coatings. a) AZ31BHF24h b) AZ31BHF72h c) WE43HF24h d) WE43HF72h e) ZM21HF24h f) ZM21HF72h g) Elemental analysis on the formed layer of AZ31B72h 253x392mm (300 x 300 DPI)

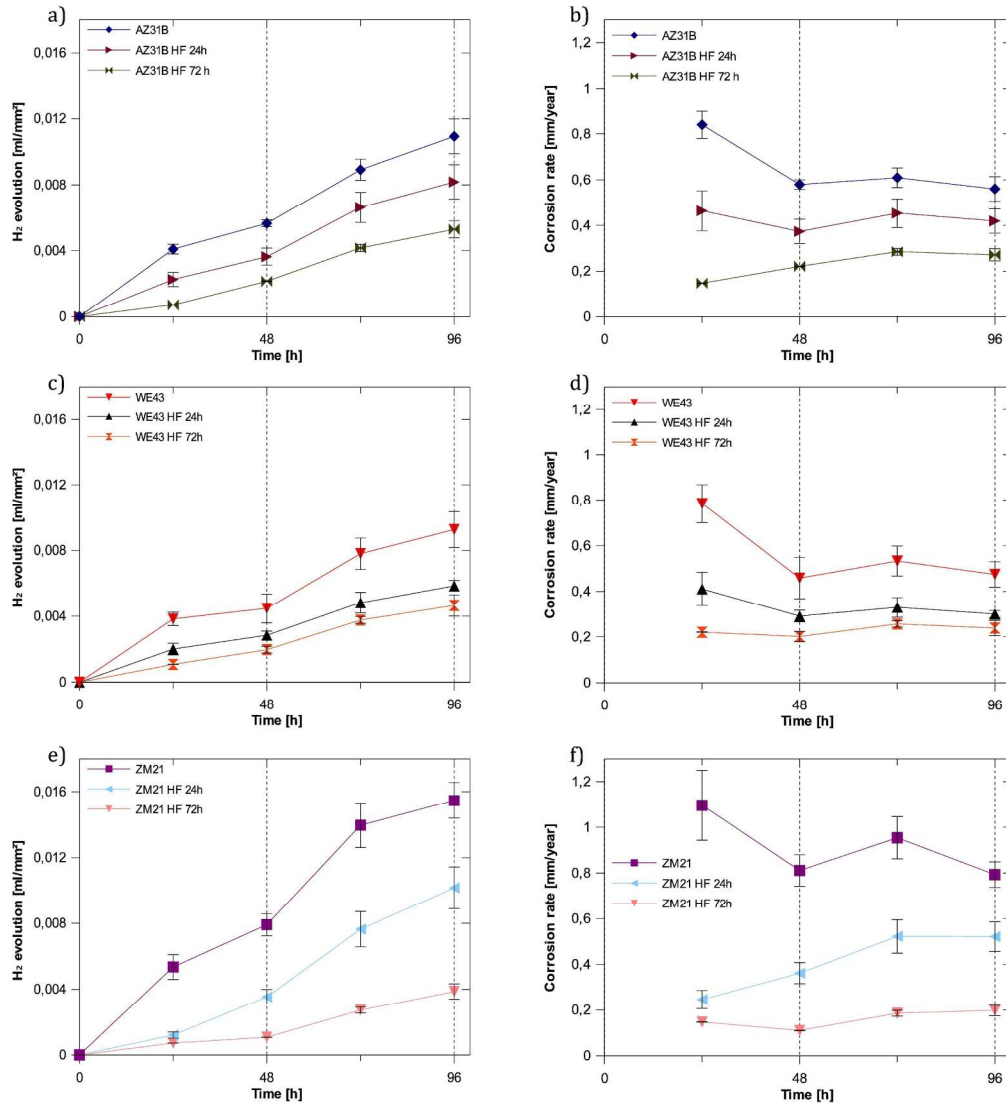


Figure 2: Hydrogen evolution and corrosion rate of, a) b) AZ31B, c) d) WE43 and, e) f) ZM21 197x216mm (300 x 300 DPI)

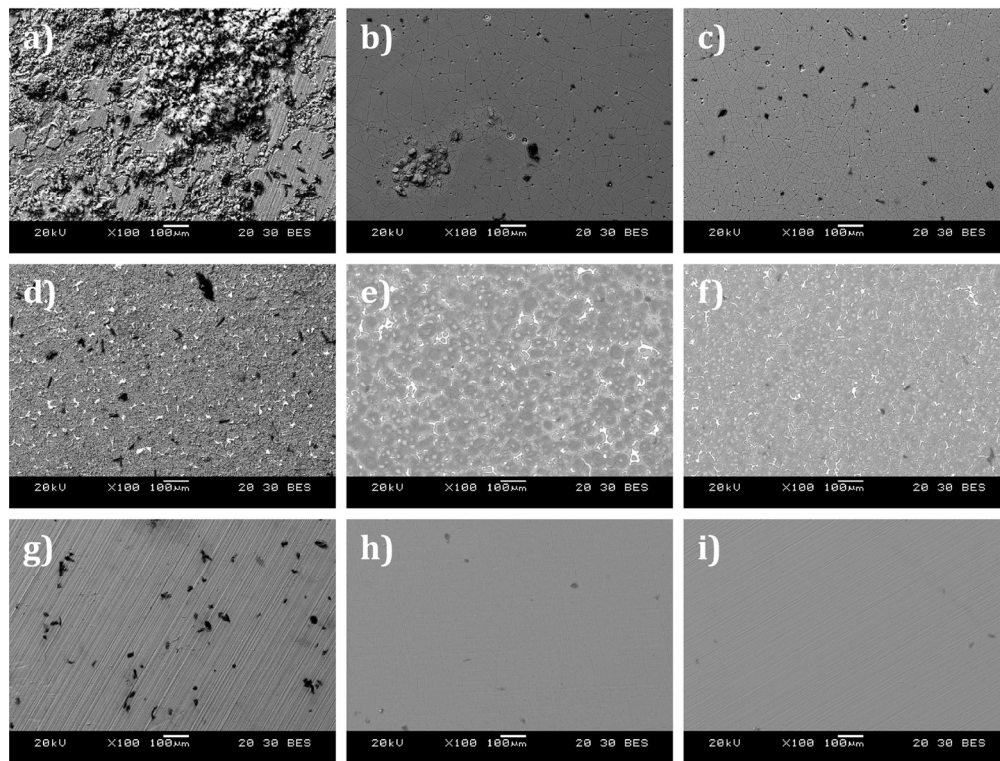


Figure 3: Surface of the samples after 72 h in PBS a) AZ31B b) AZ31BHF24h c) AZ31BHF72h d) WE43 e) WE43HF24h f) WE43HF72h g) ZM21 h) ZM21HF24h i) ZM21HF72h
139x105mm (300 x 300 DPI)

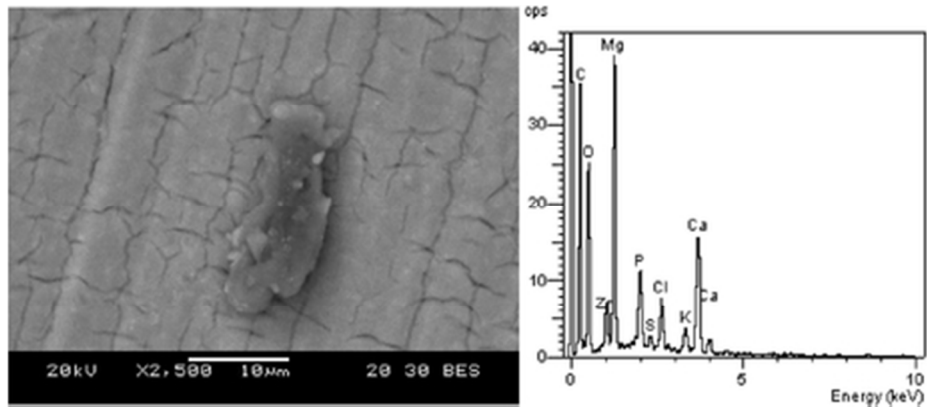


Figure 4: Deposition on ZM21 alloy after 72 hours in PBS
39x16mm (300 x 300 DPI)

Peer Review

1
2
3
4
5
6
7
8
9
10
11
12
13
14
15
16
17
18
19
20
21
22
23
24
25
26
27
28
29
30
31
32
33
34
35
36
37
38
39
40
41
42
43
44
45
46
47
48
49
50
51
52
53
54
55
56
57
58
59
60

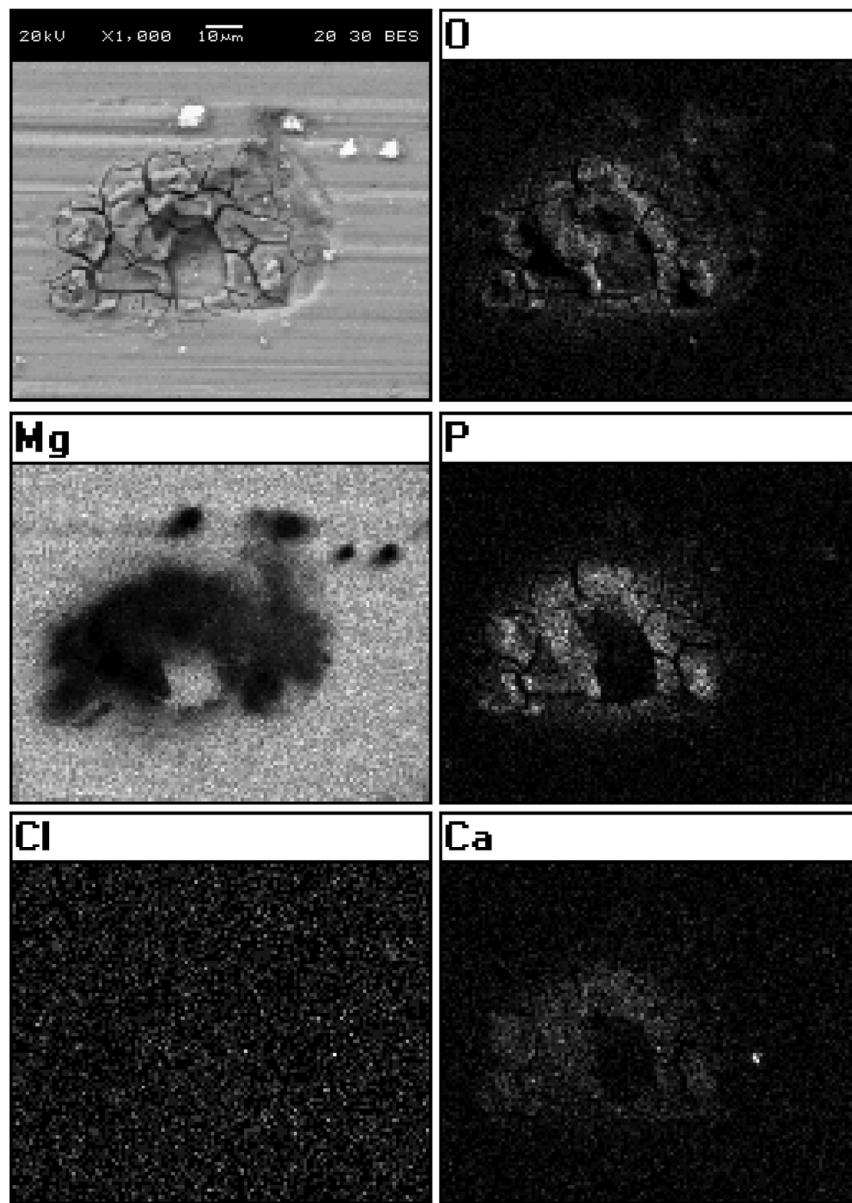


Figure 5: Element mapping of O, Mg, P, Cl and Ca on AZ31B sample after 24 hours in PBS
119x166mm (300 x 300 DPI)

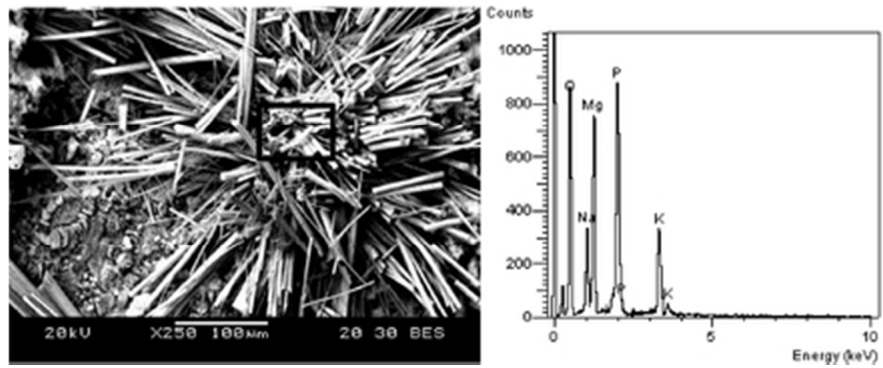


Figure 6: Needle-like depositions on AZ31B alloy after 7 days in PBS
36x15mm (300 x 300 DPI)

1
2
3
4
5
6
7
8
9
10
11
12
13
14
15
16
17
18
19
20
21
22
23
24
25
26
27
28
29
30
31
32
33
34
35
36
37
38
39
40
41
42
43
44
45
46
47
48
49
50
51
52
53
54
55
56
57
58
59
60

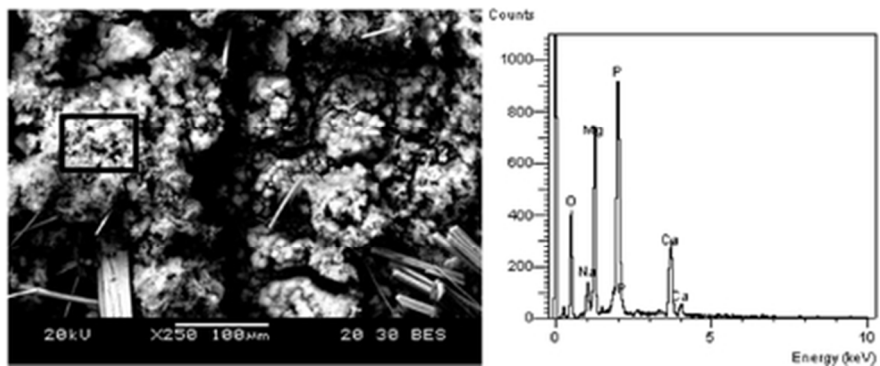


Figure 7: Sponge-like depositions on AZ31B alloy after 7 days in PBS 36x15mm (300 x 300 DPI)

Peer Review

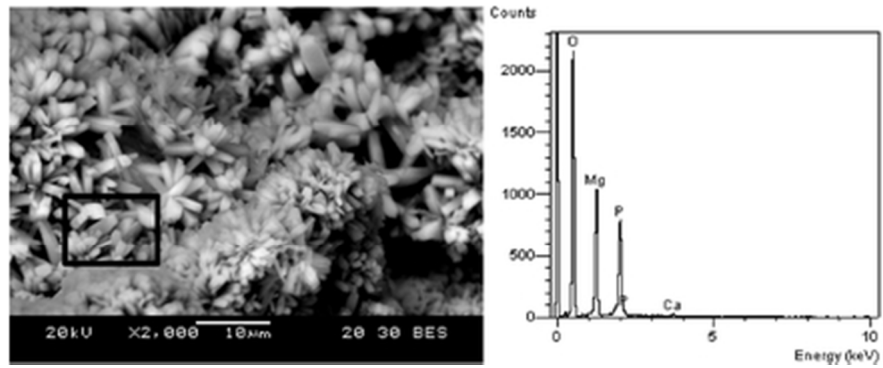


Figure 8: Formations on ZM21 alloys after 7 days in PBS
36x15mm (300 x 300 DPI)

1
2
3
4
5
6
7
8
9
10
11
12
13
14
15
16
17
18
19
20
21
22
23
24
25
26
27
28
29
30
31
32
33
34
35
36
37
38
39
40
41
42
43
44
45
46
47
48
49
50
51
52
53
54
55
56
57
58
59
60

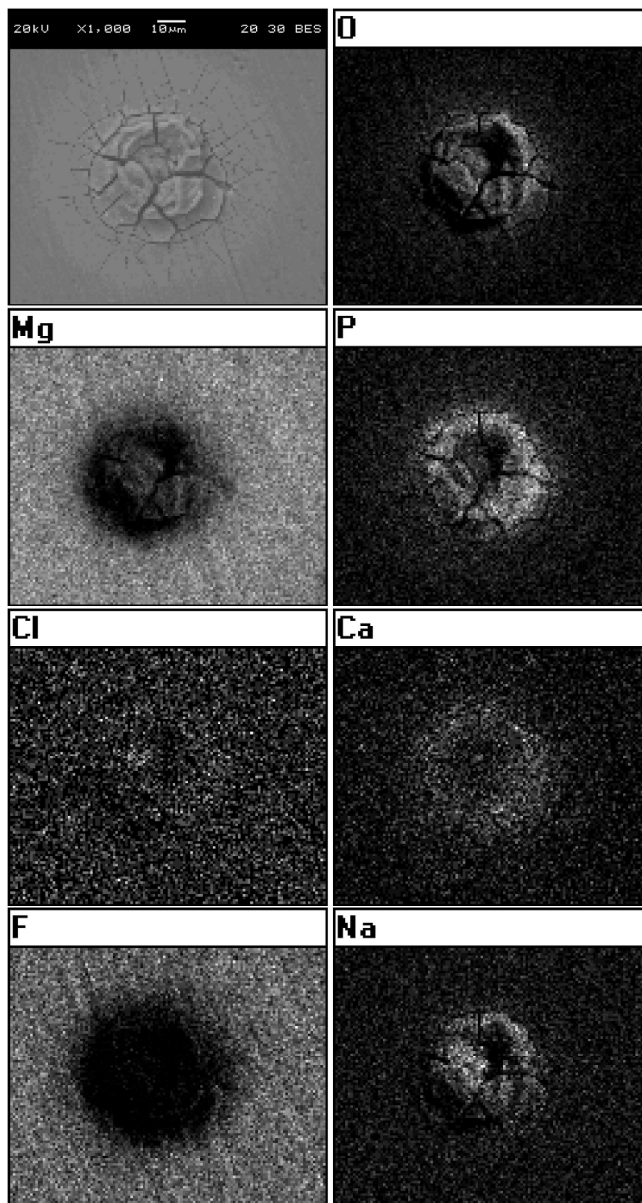
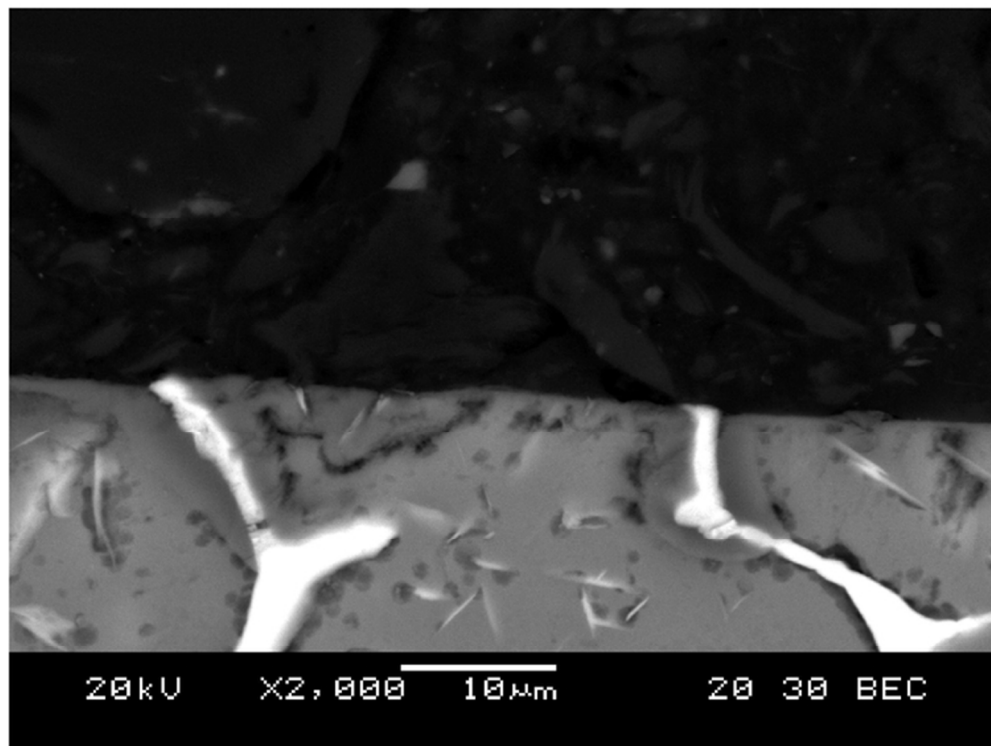


Figure 9: Element mapping of O, Mg, P, Cl, Ca, F and Na on AZ31BHF24h sample after 24 hours in PBS
157x292mm (300 x 300 DPI)



32 Figure 10: Detail of the MgF₂ around the intermetallics in the WE43 alloy
33 64x48mm (300 x 300 DPI)
34
35
36
37
38
39
40
41
42
43
44
45
46
47
48
49
50
51
52
53
54
55
56
57
58
59
60

1
2
3
4
5
6
7
8
9
10
11
12
13
14
15
16
17
18
19
20
21
22
23
24
25
26
27
28
29
30
31
32
33
34
35
36
37
38
39
40
41
42
43
44
45
46
47
48
49
50
51
52
53
54
55
56
57
58
59
60

Table 1: Nomenclature of the samples

sample	alloy	coating treatment
AZ31B	AZ31B	-
AZ31BHF24h	AZ31B	24 h immersed in HF
AZ31BHF72h	AZ31B	72 h immersed in HF
WE43	WE43	-
WE43HF24h	WE43	24 h immersed in HF
WE43HF72h	WE43	72 h immersed in HF
ZM21	ZM21	-
ZM21HF24h	ZM21	24 h immersed in HF
ZM21HF72h	ZM21	72 h immersed in HF

Table 2: pH variation in the immersion test

Sample	0 h	24 h	48 h	medium change	72 h	96 h
AZ31B	7.4	7.6	7.8	7.4	7.6	7.8
AZ31BHF24h	7.4	7.7	7.8	7.4	7.78	7.9
AZ31BHF72h	7.4	7.6	7.7	7.4	7.8	7.85
WE43	7.4	7.6	7.9	7.4	7.58	7.78
WE43HF24h	7.4	7.6	7.64	7.4	7.6	7.8
WE43HF72h	7.4	7.63	7.84	7.4	7.64	7.8
ZM21	7.4	7.72	7.96	7.4	7.78	7.93
ZM21HF24h	7.4	7.72	7.82	7.4	7.74	7.8
ZM21HF72h	7.4	7.6	7.6	7.4	7.68	7.8

Table 3. Comparison of the corrosion rates of the present work with the literature

	r_{corr} [mm year ⁻¹]	Electrolyte	Characterization test	Ref.
AZ31B	0.56	PBS	Immersion test	Present work
	12.52	PBS	Potentiodynamic polarisation	[69]
	1.425	SBF	Potentiodynamic polarisation	[38]
	8.965	SBF	Potentiodynamic polarisation	[60]
	0.711	Hank's solution	Potentiodynamic polarisation	[70]
	0.323	Hank's solution	Immersion test	[70]
	0.672	-	<i>In vivo</i>	[70]
	0.3	Hank's solution	Immersion test	[71]
	0.709	0 mol NaCl l ⁻¹	Potentiodynamic polarisation	[54]
	294	10 ⁻⁵ mol NaCl l ⁻¹	Potentiodynamic polarisation	[54]
	0.505	10 ⁻⁴ mol NaCl l ⁻¹	Potentiodynamic polarisation	[54]
	0.914	10 ⁻³ mol NaCl l ⁻¹	Potentiodynamic polarisation	[54]
	1.395	10 ⁻² mol NaCl l ⁻¹	Potentiodynamic polarisation	[54]
	1.740	10 ⁻¹ mol NaCl l ⁻¹	Potentiodynamic polarisation	[54]
	0.284	SBF	Potentiodynamic polarisation	[50]
	1.152	0 mol NaCl l ⁻¹ saturated with CO ₂	Potentiodynamic polarisation	[54]
	1.079	10 ⁻⁵ mol NaCl l ⁻¹ saturated with CO ₂	Potentiodynamic polarisation	[54]
	1.547	10 ⁻⁴ mol NaCl l ⁻¹ saturated with CO ₂	Potentiodynamic polarisation	[54]
	3.778	10 ⁻³ mol NaCl l ⁻¹ saturated with CO ₂	Potentiodynamic polarisation	[54]
	5.178	10 ⁻² mol NaCl l ⁻¹ saturated with CO ₂	Potentiodynamic polarisation	[54]
8.096	10 ⁻¹ mol NaCl l ⁻¹ saturated with CO ₂	Potentiodynamic polarisation	[54]	
6.597	Hank's solution	Potentiodynamic polarisation	[72]	
0.25	Hank's solution	Immersion test	[73]	
0.098	Hank's solution	Potentiodynamic polarisation	[73]	
0.737	m-SBF	Potentiodynamic polarisation	[74]	
0.522	m-SBF	Potentiodynamic polarisation	[74]	
8.29	m-SBF	Immersion test	[74]	
1.997	m-SBF	Immersion test	[74]	
WE43	0.47	PBS	Immersion test	Present work
	1.2	SBF	Potentiodynamic polarisation	[60]

1
2
3
4
5
6
7
8
9
10
11
12
13
14
15
16
17
18
19
20
21
22
23
24
25
26
27
28
29
30
31
32
33
34
35
36
37
38
39
40
41
42
43
44
45
46
47
48
49
50
51
52
53
54
55
56
57
58
59
60

	0.704	-	<i>In vivo</i>	[56]
	1.44	-	<i>In vivo</i>	[56]
	0.361	SBF	Potentiodynamic polarisation	[58]
	4.467	SBF	Immersion test	[58]
	0.035	SBF	Immersion test	[64]
	4.221	SBF	Immersion test	[70]
	0.896	-	<i>In vivo</i>	[70]
<hr/>				
ZM21	0.79	PBS	Immersion test	Present work
	0.919	SBF	Potentiodynamic polarisation	[60]
	0.939	Ringer solution	Potentiodynamic polarisation	[59]
	0.004	Ringer solution	Potentiodynamic polarisation	[59]

For Peer Review

List of changes

The changes made to the reference JEIM1468 are listed below:

- The abstract has been reduced to 100 words.
- The organization of the paper has been improved.
- The use of the Piiper et al model has been dismissed to evaluate the hydrogen evolution.
- Reviews and more recent papers on the measurement of Mg corrosion has been included.

Experimental methods

- The conversion coating process has been explained in more detail.

Results

- Figure 1 has been presented at higher magnifications to observe the layer in more detail.
- The MgF₂ conversion layer grown on each alloy has been described. The thickness reached on each alloy and time of treatment has been indicated.

- The composition of the MgF_2 layer has been analysed by EDX in order to demonstrate the composition of the layer.
- Symbols of the Figure 2 have been enlarged.
- A better explanation of Figure 2 has been made. The reason of supply the corrosion rate graphs in addition to the hydrogen evolution was also justified.
- The depositions and the corrosion products analysis have been improved. More studies at higher magnifications with mapping and elemental analysis have been made in order to understand the corrosion of the magnesium alloys and the protection of the coating.

Discussion

- A comparison has been made with the data of the table III and with the results of the present work.
- The summary figure about the corrosion of the samples has been removed.
- To explain the increase of the corrosion resistance in WE43 despite having a non-uniform and barely perceptible coating a possible explanation has been exposed.

- The possible composition of the depositions and corrosion products has been discussed.

Conclusions

- Conclusions have been numbered as a list of short conclusions.